

# Cellular considerations for optimizing bone cell culture and remodeling in a lab-on-a-chip platform

Sharon L Truesdell\*<sup>1</sup>, Estee L George<sup>1</sup> & Marnie M Saunders<sup>1</sup>

## ABSTRACT

Our lab has developed a lab-on-a-chip platform for bone remodeling that enables long-term culturing of bone cells out to 7 weeks and serves as a foundation toward a multicellular organ-on-a-chip system. Here, we optimized culturing protocols for osteoblasts, osteoclasts and osteocytes within the lab-on-a-chip and performed functional activity assays for quantifying bone formation and resorption. We analyzed cell seeding densities, feeding schedules and time in culture as a basis for optimizing culturing protocols. Further, we addressed concerns of sterility, cytotoxicity and leakage during the extended culture period within the polydimethylsiloxane chip. This system provides a method for quantifying the soluble effects of mechanically stimulated osteocytes on bone remodeling (formation/resorption).

## METHOD SUMMARY

Methods of culturing bone cells out to 7 weeks within a lab-on-a-chip platform have been optimized and allow for quantification of bone remodeling functional activity (formation/resorption) and soluble effects of mechanical loading.

## KEYWORDS

bone remodeling • lab-on-a-chip • osteoblasts • osteoclasts • osteocytes • polydimethylsiloxane

<sup>1</sup>Department of Biomedical Engineering, The University of Akron, Akron, OH 44325, USA;

\*Author for correspondence: [slt79@zips.uakron.edu](mailto:sbt79@zips.uakron.edu)

Bone is a dynamic tissue that is sensitive to its mechanical environment and can adapt its structure in response to changes in physical stimuli. This process, known as bone remodeling, is controlled by complex multicellular interactions between osteocytes (mechanosensing cells), osteoclasts (bone resorbing cells) and osteoblasts (bone forming cells). Bone cells are reactive to a variety of mechanical stimuli including fluid shear stress, direct cell strain, hydrostatic pressure and hoop strain [1–3], though evidence suggests that fluid shear stress and direct cell strain are likely the dominant mechanisms for inducing mechanotransduction [4].

*In vivo*, osteocytes reside within the lacunar–canalicular system of the bone matrix. It is estimated that within the tight confines of the canaliculi, interstitial fluid flow induces shear stresses up to 5 Pa on osteocyte cell processes [5]. Within the wider lacunar space, the osteocyte body is exposed to considerably lower levels of shear stress that may not be sufficient to induce a response [6,7]. In contrast, direct cell strain appears to stimulate stretch ion channels on the osteocyte cell body and has less significant effects on cellular processes [8]. However, little is known about specific ion channels on osteocytes that induce mechanoresponses [4].

Various *in vitro* models have been developed to investigate bone remodeling, yet most of these studies analyze individual cell types in isolation; more comprehensive investigations of bone metabolic pathways require multicellular models. In recent years, lab-on-a-chip (LOC) technology has progressed rapidly, leading to a variety of multicellular organ-on-a-chip platforms that replicate the physiologic milieu [9–11]. With the anticipated usefulness of this technology for drug discovery, it has been recognized that these systems must do more than faithfully recapitulate observable organ features [12]. For bone, this usefulness includes the ability to incorporate the

complexities of multicellular interactions (osteocytes, osteoclasts and osteoblasts) with the ability to respond to physiologic stimuli. The response must ultimately be measurable with the quantification of bone resorption and formation.

Although the bone field has yet to develop a true organ-on-a-chip, many microfluidic systems have been developed that incorporate some of the complexities of the bone microenvironment. Kou *et al.* developed a microfluidic device that exposes osteoblasts to four separate fluid-induced shear stress profiles [13]. Middleton *et al.* designed a co-culture system to investigate cell–cell communication between osteocytes and osteoclasts exposed to different levels of fluidic shear stress [14]. Additional systems have been developed to recreate the 3D structure of the lacunar–canalicular system [15,16]. While many of the current microfluidic systems use fluid flow to induce mechanotransduction, our focus is on understanding the effects of direct cell strain. Additionally, whereas many current bone-related devices assess functional activity indirectly, our goal is to directly quantify formation and resorption. However, this requires a culturing system that can be maintained on the order of weeks to months.

To that end, our lab has developed a LOC platform for bone remodeling that serves as a foundation toward a multicellular organ-on-a-chip that will model the physiologic microenvironment of bone. The goal of the current design is to serve as a proof-of-concept device for developing long-term culturing protocols that maintain cell viability, typical morphology and functional activity within a polydimethylsiloxane (PDMS) environment for all three bone cell types. Wei *et al.* developed a microfluidic device to assess the effects of surface modification and channel dimensions on osteocyte proliferation and morphology [17]. However, in their system, osteocytes are grown on glass substrates; for our purposes, osteocytes must be cultured on deformable PDMS membranes

to allow for mechanical load application. Several LOC configurations were developed for enabling long-term culture and quantification of functional activity for osteoblasts and osteoclasts and for stimulating osteocytes with direct cell strain [18,19]. Osteocyte stimulation was accomplished by pairing the LOC with a 3D-printed loading device (previously described) to stretch the PDMS membrane on which the osteocytes were grown [20]. Here we describe the optimization of cell culturing protocols for osteoblasts, osteoclasts and osteocytes within the LOC system. Long-term culturing, out to 7 weeks, in the LOC presents unique challenges. Further, we address concerns of sterility, cytotoxicity and chip leakage.

## MATERIALS & METHODS

### Fabrication of LOC platforms

Chip masks (Figure 1A) were fabricated using high-resolution stereolithography (Protolabs, MN, USA). The top mask consists of three different configurations containing either one or three wells each. The bottom mask was designed by modifying the single well configuration to accommodate a mechanical loading device developed by our lab [20]. The well diameter and depth were increased to allow for loading and channel depths were increased to allow for faster fluid administration. Schematic drawings of chips generated from these two masks are shown in Figure 1B. Chips were made from PDMS using a 10:1 ratio of elastomer base to curing agent (Dow Corning Sylgard 184 Silicone Elastomer). The polymer was mixed vigorously, placed in a vacuum desiccator, slowly poured over a level mask and cured for 18 h at 45°C. After curing, individual chips were cut using a scalpel. PDMS lids (3 mm thick) were generated in a similar manner and access holes were created in them with a biopsy punch (1 mm diameter). Chips and lids were plasma oxidized (Plasma Cleaner, Harrick Plasma) for 30 s using a medium RF power setting (200 mTorr, 10 W). After careful alignment, the two pieces were firmly pressed together and baked for 10 min at 65°C to increase the bond strength. Angled dispensing tips (18-gauge, 0.5", 90°) were inserted into the access holes in the lids and secured with Loctite® two-part epoxy. The outsides of the chips were disinfected with 70% ethanol and exposed to UV light (254 nm, 240 µW/cm<sup>2</sup>) for 30 min inside a

biosafety cabinet, approximately 60 cm from the light source. Sterile Tygon tubing (1/32" ID) was used to connect the dispensing tips to a 5-ml syringe equipped with an 18-gauge needle. All fluids were administered using a syringe pump (Pico Plus, Harvard Apparatus) set to a flow rate of 4 ml/h. Wells and channels were disinfected with 70% ethanol and washed three-times with sterile dH<sub>2</sub>O to thoroughly remove trace amounts of ethanol.

### Bone formation analysis

Bone formation studies were performed on tissue culture (TC)-treated polystyrene discs that were fixed to the bottom of the chip wells prior to assembly (Figure 1C). The polystyrene discs were cut from TC-treated coverslips. The non-TC-treated side was marked with masking tape and individual discs were cut using a 5.4-mm cork-borer. Discs were soaked in 70% ethanol overnight and cleaned of debris and tape residue with a Q-tip soaked in ethanol. Discs were attached to the bottom of the well (TC-treated side up) with a thin layer of uncured PDMS, left at room temperature overnight to allow for even spreading of the PDMS and baked at 65°C for at least 2 h. Following chip fabrication, MC3T3-E1 murine preosteoblasts (ATCC, VA, USA) were seeded at a flow rate of 5 ml/h on TC-treated polystyrene discs in MEM-α (Gibco, Thermo Fisher Scientific, MA, USA) supplemented with 10% FBS (Hyclone, GE Healthcare Life Sciences, NJ, USA) and 1% penicillin/streptomycin (Invitrogen, Thermo Fisher Scientific, MA, USA) and maintained in 5% CO<sub>2</sub> at 37°C. At 100% confluence, cells were induced to differentiate with 10-mM β-glycerophosphate and 50 µg/ml L-ascorbic acid in culture medium. Throughout the culturing period, cells were fed every 72 h by pushing fresh medium through the chip with a syringe pump at a flow rate of 2 ml/h until 100% of the medium was replaced. To increase mineralization, the following variables were analyzed: cell seeding density, feeding schedule and time in culture. For end point analysis, the bone wafers were removed from the chip and resorption was quantified with a toluidine blue stain. Osteoclasts were removed from the wafers with 30 min of sonication in 70% isopropanol, followed by gentle rubbing with a Q-tip. Wafers were submerged in a 1% toluidine blue solution for 5 min, rinsed with dH<sub>2</sub>O, stained a second time for 2 min and rinsed with dH<sub>2</sub>O. The percentage area covered with resorption pits was determined using ImageJ.

spatula (if the monolayer was adhered to the side of the PDMS well, a scalpel was used to release it). The polystyrene disc was then placed on a clean glass slide and imaged. Percentage area of bone formation was determined using NIH ImageJ [21,22].

### Bone resorption analysis

Bone resorption studies were performed on cortical bovine bone wafers (6 mm diameter, 0.4 mm thick, Boneslices.com, Jelling, Denmark) fixed to the bottom of each well, following the same protocol used for the polystyrene discs. After chip fabrication, bone wafers were rinsed with HBSS and rehydrated in DMEM (Corning, NY, USA) supplemented with 10% FBS and 1% penicillin/streptomycin for at least 3 h. Murine RAW 264.7 preosteoclast cells (ATCC) were seeded at a flow rate of 5 ml/h on bone wafers in DMEM supplemented with 10% FBS and 1% penicillin/streptomycin and maintained in 5% CO<sub>2</sub> at 37°C. At 24 h, cell differentiation was induced with 120 ng/ml RANKL in culture medium. Throughout the culturing period, cells were fed every 72 h by pushing fresh medium through the chip with a syringe pump at a flow rate of 2 ml/h until 100% of the medium was replaced. To increase resorption, the following variables were analyzed: cell seeding density, feeding schedule and time in culture. For end point analysis, the bone wafers were removed from the chip and resorption was quantified with a toluidine blue stain. Osteoclasts were removed from the wafers with 30 min of sonication in 70% isopropanol, followed by gentle rubbing with a Q-tip. Wafers were submerged in a 1% toluidine blue solution for 5 min, rinsed with dH<sub>2</sub>O, stained a second time for 2 min and rinsed with dH<sub>2</sub>O. The percentage area covered with resorption pits was determined using ImageJ.

### Osteocyte protocols

For mechanical loading studies, the modified single-well chip configuration was utilized. The chip was formed from two separate pieces, the bottom of the well being generated by attaching a PDMS membrane (0.5 mm thick) to the bottom of the chip using plasma oxidation (Figure 1D). This minimized warping of the membrane during the curing process. Chips were fabricated as previously described, with the following modifications: channels and wells were

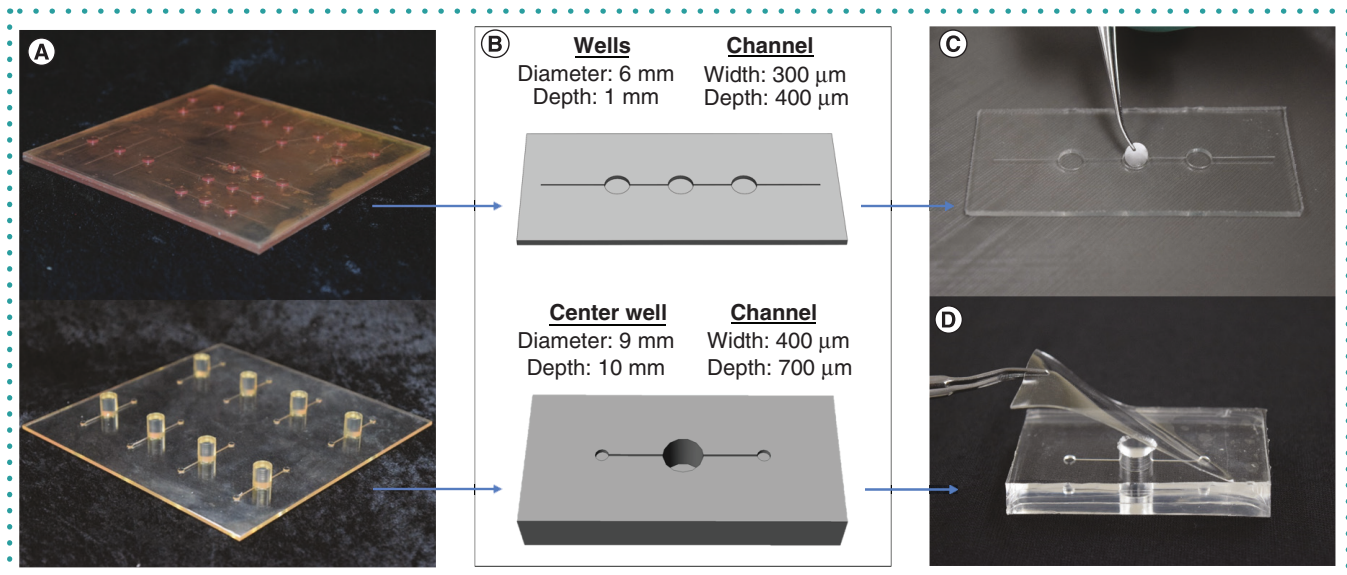


**Figure 1.** Lab-on-a-chip configurations. (A) Chip masks. (Top) Mask consisting of three different configurations containing either one or three wells each. (Bottom) Mask consisting of a single well design with increased dimensions to accommodate mechanical loading. (B) Schematic drawings of PDMS chips generated from each of the chip masks. (C) For osteoblast cultures, a polystyrene disc was attached to the bottom of each well prior to sealing the chip with a lid. (D) Thicker chips were generated from two separate pieces. The bottom of each well was formed by attaching a separate 0.5 mm-thick PDMS membrane to the bottom of the chip. PDMS: Polydimethylsiloxane.

disinfected with 70% ethanol, exposed to UV light (254 nm, 240  $\mu\text{W}/\text{cm}^2$ ) overnight inside a biosafety cabinet, approximately 60 cm from the light source, rinsed three-times with sterile  $\text{dH}_2\text{O}$ , filled with sterile  $\text{dH}_2\text{O}$  and incubated for a minimum of 48 h. Wells were then coated with collagen type I (CTI, BD Biosciences, NJ, USA) for 1 h, rinsed three-times with DPBS with calcium and magnesium and seeded with murine osteocytic MLO-Y4 cells (a generous gift from Dr Lynda Bonewald) at 20,000 cells/ml in MEM- $\alpha$  supplemented with 5% calf serum (Hyclone), 5% FBS and 1% penicillin/streptomycin; cultures were maintained at 5%  $\text{CO}_2$  and 37°C. At 72 h, cells were imaged to ensure typical morphology. Once typical cell morphology is obtained, osteocytes can be subjected to mechanical stimulation via direct cell strain. We have previously described a 3D-printed loading device that can be paired with our LOC platform [20]. This device, which works like a screw jack, stretches the PDMS membrane on which the cells are seeded by tenting the material from below.

## RESULTS & DISCUSSION

The development of a LOC for culturing osteoblasts, osteoclasts and osteocytes posed a variety of challenges, which we have addressed in the protocols described here.

In addition to optimizing our standard culturing protocols for each cell type within the system, we have addressed concerns of sterility, toxicity and leakage during this extended culture period.

### Alterations in culturing protocols

#### Osteoblasts

Within traditional culture plates, we have previously demonstrated that MC3T3-E1 osteoblasts significantly increase mineral deposition by day 26 (Table 1) [23]. A summary of the parametric culturing protocols within the LOC (1.0  $\text{mm}^{-1}$  surface area to volume ratio) is provided in Table 1. Originally, evaporation within this system was a concern; for this reason, we began with a daily feeding regimen. We found that feedings could be extended to every 2 and 3 days with minimal medium losses. We determined that a higher seeding density (10,000 cells/ $\text{cm}^2$ ) was required for the cells to reach 100% confluence. Further, a longer time in culture (49 days) was required before mineralization was detected. We believe this may be due to a reduction in paracrine signaling within the LOC system. Traditional feedings are performed by replacing 50% of the culture medium; however, cells within the LOC are fed by replacing 100% of the culture medium. We are currently working on an automated feeding system that will

allow feedings with 50% replacement to be administered reproducibly.

Protocol alterations were also made to ensure attachment of the cell monolayer to the polystyrene discs. Figure 2A shows the nonadherence of the osteoblast layer near the edge of the disc by day 18. We ideally wanted to avoid the need of a surface protein to achieve cell attachment; however, we attempted coating the polystyrene disc with fibronectin prior to cell seeding. While this may have increased early cell adherence, by day 49, cell adherence was still low (Figure 2B). Ultimately, we found that decreasing the flow rate used during feeding to 2 ml/h was sufficient to maintain cell attachment throughout the culture period. Representative images of MC3T3-E1 cells at 49 days using this method are shown in Figure 2C. Mineralization was detected with both alizarin red and von Kossa stains.

#### Osteoclasts

We previously demonstrated that within 96-well plates, RAW 264.7 preosteoclasts seeded on bone wafers could be induced to resorb bone by day 20 (Table 2) [19]. However, within the LOC, the same volumetric seeding density (5000 cells/ml) resulted in minimal bone resorption even at day 30. This is likely due to the decreased volume of fluid within ▶

**Table 1. Culture conditions for osteoblasts in traditional cell culture plates and tested conditions on polystyrene discs within the lab-on-a-chip.**

**Osteoblasts in traditional cell culture plates**

Density	Feedings	Time in culture	Observations
2500 cells/cm <sup>2</sup>	Every 72 h	26 days	Mineralization detected via alizarin red and von Kossa stains covered an average of 20.6 and 20.5% of the surface area, respectively [23]

**Osteoblasts on polystyrene discs in LOC**

Density	Feedings	Time in culture	Observations
2500 cells/cm <sup>2</sup>	Every 24 h	30 days	
10,000 cells/cm <sup>2</sup>	Every 72 h	32 days	Minimal mineralization detected via alizarin red stain
		35 days	
		39 days	Minimal mineralization detected via alizarin red and von Kossa stains
		49 days	Mineralization detected via alizarin red and von Kossa stains covered an average of 10.72 and 6.43% of the surface area, respectively [19]

LOC: Lab-on-a-chip.

each well, resulting in a decrease in total cells. A summary of the parametric culturing

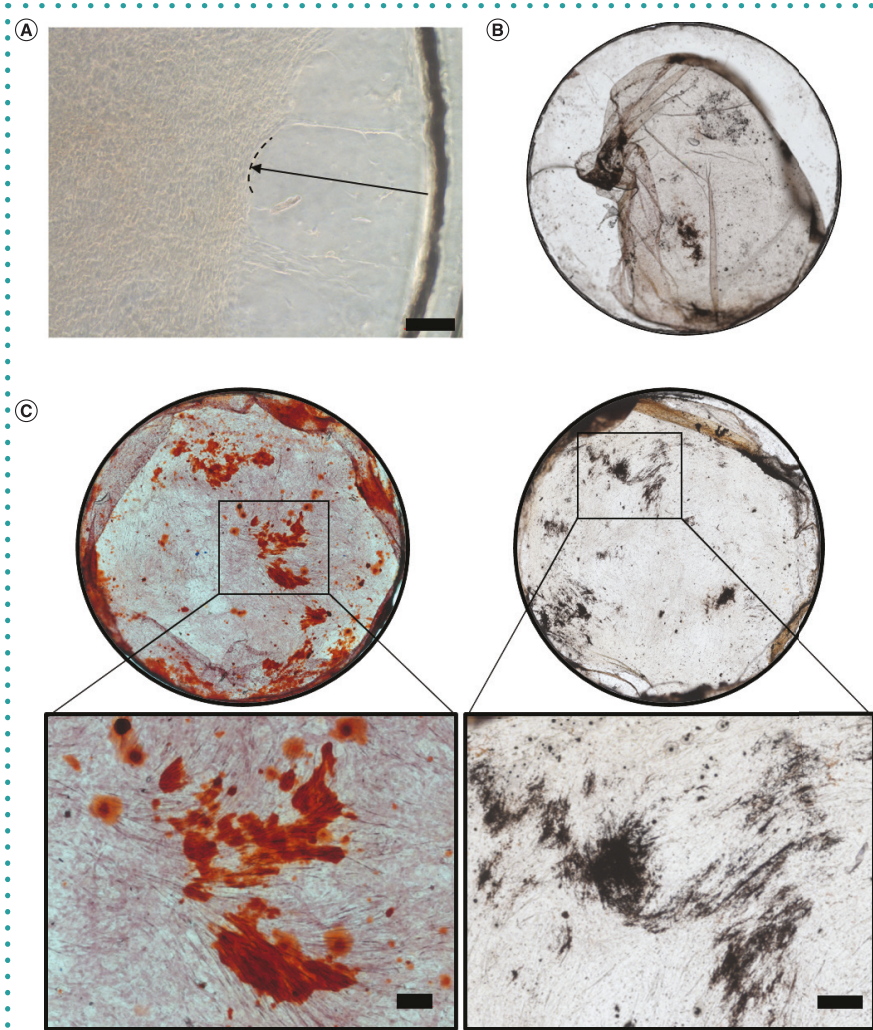


**Figure 2. Osteoblast results.** (A) MC3T3-E1 osteoblasts on polystyrene discs showed a decrease in cell adherence by day 18. The dashed line indicates the edge of the cell monolayer and the arrow indicates the regression of the monolayer from the edge of the polystyrene disc. (B) Application of a fibronectin coating to the polystyrene disc was insufficient for maintaining osteoblast monolayer adhesion through end point analysis at day 49. (C) Typical results of mineralization detected via alizarin red (left) and von Kossa (right) staining at day 49 using optimized protocol. Scale bars represent 200  $\mu$ m. Whole polystyrene disc images measure 5.4 mm in diameter.

protocols within the LOC (1.7 mm<sup>-1</sup> surface area to volume ratio) is provided in Table 2. Again, we began with a daily feeding regimen, but found that this could be extended to every 2 or 3 days with minimal medium losses. Additionally, we found that increasing the seeding density to 1500 cells per well resulted in a similar amount of resorption when compared with traditional culture plates. A seeding density of 56,000 cells per well was also analyzed; the resulting resorption was not significantly different from that seen with a density of 1500 cells per well.

Further, we found that detection of resorption pits required a second staining in the toluidine blue solution for 2 min. Figure 3A shows bone wafers following one and two staining periods; after the second round of staining, pit formation is much more clearly defined. The lack of pit detection on a control wafer ensured that positive results were not an artifact from increased stain exposure time. Pit formation was also confirmed with scanning electron microscopy (Figure 3B). Ultimately, we found that within the LOC, a seeding density of 1500 cells per well with feeding every 3 days for 30 days was sufficient for detecting resorption via toluidine blue stain. Representative results are shown in Figure 3C.

#### Osteocytes

To investigate the effects of mechanical load on osteocytes, we modified the single-well chip configuration. MLO-Y4 osteocytes were seeded directly on a thin CTI-coated PDMS membrane. We found that osteocytes were more sensitive to PDMS fabri-

**Table 2. Culture conditions for osteoclasts on bone wafers in traditional cell culture plates and tested conditions for osteoclasts on bone wafers within the lab-on-a-chip.**

Osteoclasts on bone wafers in traditional cell culture plates					
Density	Feedings	Time in culture	Observations		
1000 cells/well (5000 cells/ml)	Every 48 h	20 days	Resorption detected via toluidine blue stain covered an average of 24.9% of the surface area [19]		
Osteoclasts on bone wafers in LOC					
Density	Feedings	Time in culture	Observations		
150 cells/well (5000 cells/ml)	Every 24 h	20 days	Minimal resorption detected via toluidine blue stain		
	Every 48 h	30 days			
1500 cells/well (50,000 cells/ml)	Every 72 h		Resorption detected via toluidine blue stain covered an average of 30.4% of the surface area [19]		
56,000 cells/well ( $\approx 1.9 \times 10^6$ cells/ml)	Every 48 h		Resorption detected via toluidine blue stain covered an average of 32.06% of the surface area		
	Every 72 h		Resorption detected via toluidine blue stain covered an average of 28.7% of the surface area [19]		

LOC: Lab-on-a-chip.

cation techniques than the other two cell types and protocol modifications were required to obtain high cell viability and typical morphology. When cells were immediately seeded within the chips ( $0.1 \text{ mm}^2$  surface area to volume ratio) following the initial fabrication protocol, a high degree of cell death was observed (Figure 4A). To overcome this issue, we incubated the fully fabricated chips for a minimum of 48 h with  $\text{dH}_2\text{O}$  at  $37^\circ\text{C}$  prior to seeding cells. While this alteration significantly improved cell viability, atypical morphologies were still observed. By 72 h, cells tended to clump (Figure 4B). We attempted several procedures to alter the surface properties of the PDMS membrane. Figure 4C shows osteocytes seeded within a chip that received an additional 30 min of plasma oxidation following the previous fabrication protocol. Cells were also seeded in chips that were autoclaved (Figure 4D); autoclaved and exposed to UV light overnight (Figure 4E); or only exposed to UV light overnight (Figure 4F). Overall, we found that cells seeded in chips exposed to UV light (with or without autoclaving) displayed high viability and typical morphology. Further, to ensure that osteocyte behavior would not be altered by PDMS material properties, our lab has previously characterized osteocyte growth and functional behavior on CTI-coated PDMS. We found that when compared with osteocytes grown on CTI-coated glass, cell proliferation was not significantly different at 48, 72, 96 or 120 h; at 120 h, osteocyte growth had increased by 257 and 222% on PDMS and glass, respectively [24]. Immunofluo-

rescent staining also confirmed that osteocytes grown on CTI-coated PDMS express key osteocyte proteins Dkk-1, RANKL, and the gap junction protein Cx43 [19,24]. Further, cell-cell communication via gap

junctions was not significantly different between the two substrates; at 72 h, the percentages of osteocytes that were in communication on PDMS and glass were 63.5 and 64.1%, respectively [24]. ▶

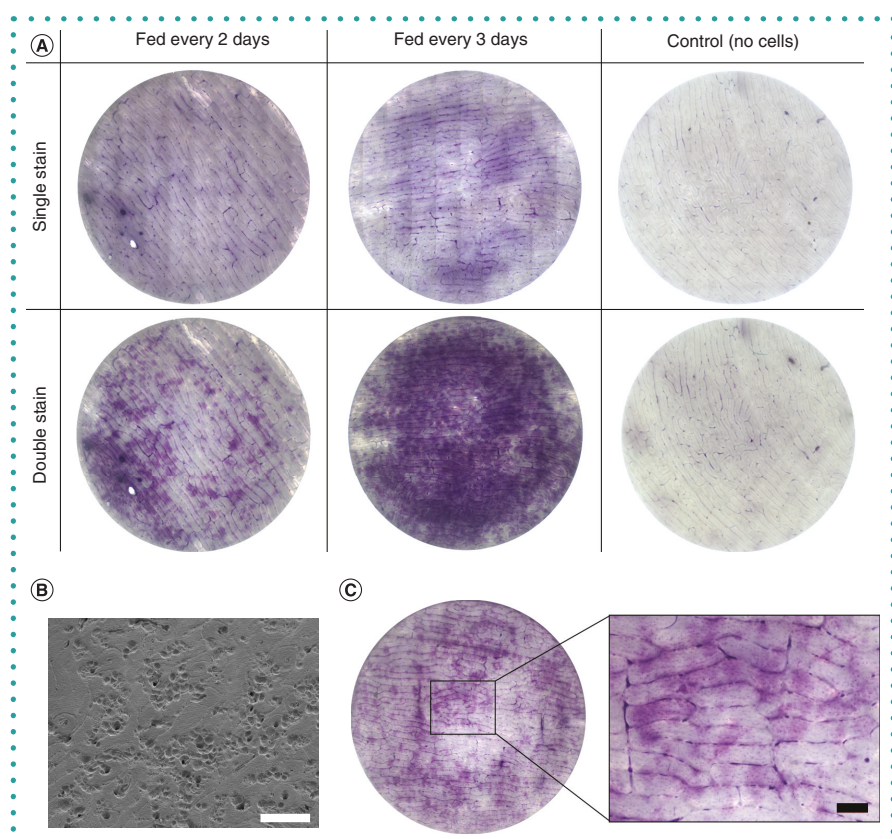


**Figure 3. Osteoclast results.** (A) Double staining bone wafers with toluidine blue enhanced visualization of resorption pits, regardless of feeding schedule. Control wafers ensured that results were not an artifact resulting from increased stain exposure. (B) Representative scanning electron microscope image of resorption pits on bone wafers at day 30. (C) Typical results of resorption detected via double toluidine blue staining of bone wafers at day 30; they were seeded at 50,000 cells/ml and fed every 3 days within the LOC. All scale bars represent 200  $\mu\text{m}$ . Whole bone wafers measure 6 mm in diameter.

LOC: Lab-on-a-chip.

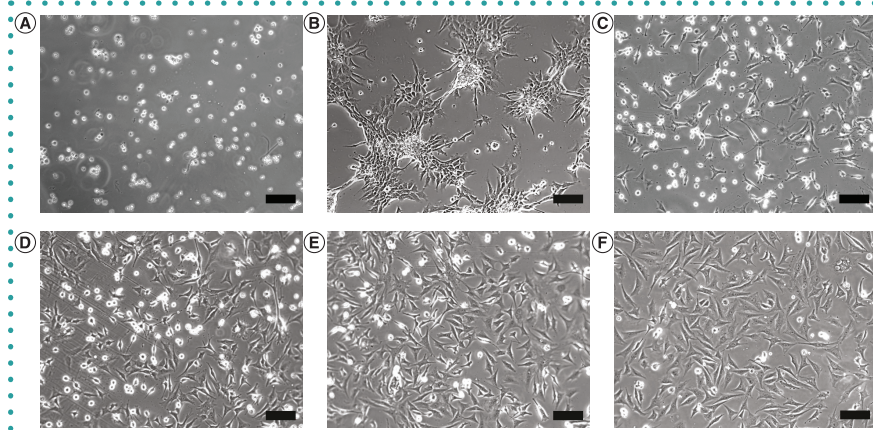


**Figure 4.** Images of MLO-Y4 osteocytes at 72 h seeded on collagen type I-coated polydimethylsiloxane membrane within the lab-on-a-chip. The following modifications to the chip fabrication protocol were tested to enhance cell viability and ensure typical morphology: (A) No modifications. (B) Chips filled with dH<sub>2</sub>O and incubated for 48 h prior to use. (C) Chips plasma oxidized for 30 min and incubated with dH<sub>2</sub>O for 48 h prior to use. (D) Chips autoclaved, exposed to UV light overnight and incubated with dH<sub>2</sub>O for 48 h prior to use. (E) Chips autoclaved, exposed to UV light overnight and incubated with dH<sub>2</sub>O for 48 h prior to use. (F) Chips exposed to UV light overnight and incubated with dH<sub>2</sub>O for 48 h prior to use. Scale bars represent 100  $\mu$ m.

►

### Sterility & toxicity issues

In developing our PDMS sterilization protocol, we analyzed the efficacies of several techniques. We found that the combination of 70% ethanol and exposure to UV light was sufficient to eliminate the risk of contamination. Additionally, we observed that exposure to UV light resulted in a higher degree of adherent cells within osteocyte cultures. The surface of PDMS is inherently hydrophobic; however, many studies have reported that UV treatment of PDMS can result in surface oxidation [25–27]. The level of oxidation increases with longer UV exposure times and can result in local chain excision. Overall, this can lead to a moderate increase in surface wettability. This may explain the increase in cell adherence, though additional studies would be required to confirm this. In addition to ethanol and UV sterilization, we assessed PDMS sterilization via autoclaving. However, we found this to be an unnecessary step that significantly increased the fabrication time.

A sterilization protocol was also established for the Tygon tubing used for liquid administration. In between uses, the tubing was washed with 70% ethanol and sterilized via autoclaving. However, we found that repeated autoclaving cycles resulted in slight cytotoxic effects from the tubing. These effects were remedied by flushing

the tubing with excess sterile dH<sub>2</sub>O prior to use.

### Leakage

Long-term cell culturing within a multilayer PDMS chip requires a tight seal between layers. Overexposure of PDMS to plasma oxidation can weaken the integrity of the bond and increase the chance of a leak forming during the seeding or feeding procedures. We found that a 10 W RF power plasma treatment for 30 s was sufficient to create a strong bond between PDMS layers. Leakage was also more likely to occur when an increased flow rate was used to seed or feed cells. We determined that a flow rate up to 5 ml/h could be used without risk of rupturing the seal. As such, this flow rate was used to seed cells; however, as previously mentioned, a decreased flow rate of 2 ml/h was used for cell feedings.

### FUTURE PERSPECTIVE

We optimized protocols for culturing osteoblasts, osteoclasts and osteocytes within our LOC system. Further, we have demonstrated that our techniques minimize cell toxicity concerns and maintain sterility long-term (out to 49 days) for culturing bone cells – a requirement for functional activity analysis. We are also currently developing an automated feeding system which, when used with our current technology, will enhance the physiologic relevance of our

system and reduce sample variability. Development of these techniques serves as a foundation for establishing a true bone remodeling organ-on-a-chip that can expand our understanding of the multicellular intricacies governing this process. Once fully established, our platform could be used to enhance our understanding of several bone-related issues, including osteoporosis, fracture healing, periprosthetic osteolysis and bone metastasis. Further, we see our device being used to test the efficacy of investigational new drugs, thus reducing the need for animal testing.

### AUTHOR CONTRIBUTIONS

MM Saunders conceived the study. SL Truesdell and EL George conducted experiments and quantified results. SL Truesdell wrote the manuscript. All authors worked on corrections to the manuscript and approved the final submission.

### FINANCIAL & COMPETING INTERESTS DISCLOSURE

This work was supported by the National Science Foundation under grant numbers CBET 1060990 and EBMS 1700299. Also, this material is based upon work supported by the National Science Foundation Graduate Research Fellowship Program under grant number 2018250692. Any opinions, findings, conclusions, or recommendations expressed in this material are those of the authors and do not necessarily reflect the views of the National Science Foundation. The authors have no other relevant affiliations or financial involvement with any organization or entity with a financial interest in or financial conflict with the subject matter or materials discussed in the manuscript apart from those disclosed.

No writing assistance was utilized in the production of this manuscript.

### OPEN ACCESS

This work is licensed under the Attribution-NonCommercial-NoDerivatives 4.0 Unported License. To view a copy of this license, visit <http://creativecommons.org/licenses/by-nc-nd/4.0/>

## REFERENCES

Papers of special note have been highlighted as: • of interest

1. Bonewald LF. The amazing osteocyte. *J. Bone Miner. Res.* 26(2), 229–238 (2011).
2. Klein-Nulend J, Bacabac RG, Bakker AD. Mechanical loading and how it affects bone cells: the role of the osteocyte cytoskeleton in maintaining our skeleton. *Eur. Cell Mater.* 24, 278–291 (2012).
3. McGarry JG, Klein-Nulend J, Mullender MG, Prendergast PJ. A comparison of strain and fluid shear stress in stimulating bone cell responses – a computational and experimental study. *FASEB J.* 19(3), 482–484 (2005).
4. Klein-Nulend J, Bakker AD, Bacabac RG, Vatsa A, Weinbaum S. Mechanosensation and transduction in osteocytes. *Bone* 54(2), 182–190 (2013).
5. Price C, Zhou X, Li W, Wang L. Real-time measurement of solute transport within the lacunar-canalicular system of mechanically loaded bone: direct evidence for load-induced fluid flow. *J. Bone Miner. Res.* 26(2), 277–285 (2011).
6. Burra S, Jiang JX. Connexin 43 hemichannel opening associated with Prostaglandin E2(2) release is adaptively regulated by mechanical stimulation. *Commun. Integr. Biol.* 2(3), 239–240 (2009).
7. Wu D, Ganatos P, Spray DC, Weinbaum S. On the electrophysiological response of bone cells using a Stokesian fluid stimulus probe for delivery of quantifiable localized picoNewton level forces. *J. Biomech.* 44(9), 1702–1708 (2011).
8. You J, Yellowley CE, Donahue HJ, Zhang Y, Chen Q, Jacobs CR. Substrate deformation levels associated with routine physical activity are less stimulatory to bone cells relative to loading-induced oscillatory fluid flow. *J. Biomech. Eng.* 122(4), 387–393 (2000).
9. Huh D, Matthews BD, Mammoto A, Montoya-Zavala M, Hsin HY, Ingber DE. Reconstituting organ-level lung functions on a chip. *Science* 328(5986), 1662–1668 (2010).
10. Powers MJ, Domansky K, Kaazempur-Mofrad MR et al. A microfabricated array bioreactor for perfused 3D liver culture. *Biotechnol. Bioeng.* 78(3), 257–269 (2002).
11. Baudoin R, Griscom L, Monge M, Legallais C, Leclerc E. Development of a renal microchip for *in vitro* distal tubule models. *Biotechnol. Prog.* 23(5), 1245–1253 (2007).
12. Kimura H, Sakai Y, Fujii T. Organ/body-on-a-chip based on microfluidic technology for drug discovery. *Drug Metab. Pharmacokinet.* 33(1), 43–48 (2018).
13. Kou S, Pan L, Van Noort D et al. A multishear microfluidic platform for quantitative analysis of calcium dynamics in osteoblasts. *Biochem. Biophys. Res. Commun.* 408(2), 350–355 (2011).
14. Middleton K, Al-Dujaili S, Mei X, Gunther A, You L. Microfluidic co-culture platform for investigating osteocyte-osteoclast signalling during fluid shear stress mechanostimulation. *J. Biomech.* 59, 35–42 (2017).
  - Details the design of a microfluidic platform that incorporates osteocytes and osteoclasts.
15. You L, Temiyasathit S, Tao E, Prinz F, Jacobs CR. 3D microfluidic approach to mechanical stimulation of osteocyte processes. *Cell. Mol. Bioeng.* 1(1), 103–107 (2008).
  - Details a microchamber system for culturing individual osteocytes in a 3D environment that mimics the *in vivo* geometry of bone.
16. Gu Y, Zhang W, Sun Q, Hao Y, Zilberman J, Lee WY. Microbeads-guided reconstruction of 3D osteocyte network during microfluidic perfusion culture. *J. Mater. Chem. B* 3(17), 3625–3633 (2015).
17. Wei C, Fan B, Chen D et al. Osteocyte culture in microfluidic devices. *Biomicrofluidics* 9(1), 014109 (2015).
  - This article details the development of one of the first microfluidic platforms to assess on-chip culturing of osteocytes.
18. George EL, Truesdell SL, Magyar AL, Saunders MM. The effects of mechanically loaded osteocytes and inflammation on bone remodeling in a bisphosphonate-induced environment. *Bone* 127, 460–473 (2019).
19. George EL, Truesdell SL, York SL, Saunders MM. Lab-on-a-chip platforms for quantification of multicellular interactions in bone remodeling. *Exp. Cell Res.* 365(1), 106–118 (2018).
20. Truesdell SL, George EL, Seno CE, Saunders MM. 3D printed loading device for inducing cellular mechanotransduction via matrix deformation. *Exp. Mech.* 59(8), 1223–1232 (2019).
21. Shah KM, Stern MM, Stern AR, Pathak JL, Bravenboer N, Bakker AD. Osteocyte isolation and culture methods. *Bonekey Rep.* 5, 838 (2016).
22. Schindelin J, Arganda-Carreras I, Frise E et al. Fiji: an open-source platform for biological-image analysis. *Nat. Methods* 9, 676 (2012).
23. George EL. *Quantifying the Roles of Stimulated Osteocytes and Inflammation in Bone Remodeling*. Doctoral dissertation, University of Akron, OH, USA (2019).
24. York SL, Arida AR, Shah KS, Sethu P, Saunders MM. Osteocyte characterization on polydimethylsiloxane substrates for microsystems applications. *J. Biomim. Biomater. Tissue Eng.* 16, 27–42 (2012).
25. Zheng F, He CQ, Fang PF et al. The surface structure of UV exposed poly-dimethylsiloxane (PDMS) insulator studied by slow positron beam. *Appl. Surf. Sci.* 283, 327–331 (2013).
26. Ye H, Gu Z, Gracias DH. Kinetics of ultraviolet and plasma surface modification of poly(dimethylsiloxane) probed by sum frequency vibrational spectroscopy. *Langmuir* 22(4), 1863–1868 (2006).
27. Efimenko K, Wallace WE, Genzer J. Surface modification of Sylgard-184 poly(dimethyl siloxane) networks by ultraviolet and ultraviolet/ozone treatment. *J. Colloid Interface Sci.* 254(2), 306–315 (2002).